Understanding the Heterogeneity in the Bandelier Tuff:

Correlations between Geophysical and Hydrologic Data

by

Michael Thomas Petersen

Submitted in partial fulfillment

of the requirements for the degree of

Master of Science in Hydrology

Department of Earth and Environmental Science

New Mexico Institute of Mining and Technology

Socorro, New Mexico, USA

June 2012

ABSTRACT

This study focuses on the correlations between hydrological and geophysical datasets in Ash-Flow Tuffs. The study is contained within the boundaries of Los Alamos National Laboratories (LANL), located on the Pajarito Plateau on the Flanks of the Jemez Mountains in North-Central New Mexico. Recent studies on Ash-Flow Tuffs have created a conceptual model where porosity and saturated hydraulic conductivity are lowest towards the center of the tuff, and higher towards the edges due to a higher degree of welding in the interior of the tuff. The degree of welding is highest towards the volcanic source. The depositional history of ash-flow tuffs of the Pajarito Plateau is somewhat complex; where the Otowi Member was deposited first, followed by a long period of erosion and sedimentary deposition referred to as the Cerro Toledo interval, and finally a deposition of multiple, thin ash-flow tuffs deposited within a very short geological time period. Core samples were obtained from varying distance from the Jemez Volcanic center, at varying depths of different ash-flow tuff units. Hydrological datasets of porosity and saturated hydraulic conductivity were measured and compared with geophysical datasets of gamma-ray and resistivity logs obtained by LANL. Porosity measurements range from 2.7 – 42.3%. Saturated hydraulic conductivity ranges from 1.52×10^{-3} to 7.82×10^{-6} cm/sec. Resistivity ranges from 65.4-470.4 ohm-m. Gamma-ray data ranges from 164.8-277.1 API. The major trends found in this study are decreasing values for both resistivity and saturated hydraulic conductivity with increasing

distance from the volcanic center. Final results in spatial distributions of data throughout the subunits do not exhibit the same trends described above in previous studies due to the rapid deposition of multiple ash-flow tuffs, which influences the welding of the unit.

To my wonderful family, Jamie and Luke, for the amazing help to help get through, and for our future.

ACKNOWLEDGEMENTS

I have many people to thank throughout the course of this project and my education. My wife Jamie has been an amazing source of support and patience, making many sacrifices, some I am sure that I may never know. My son Luke has provided countless moments of joy and motivation. My parents, Tom and Jackie, have always been there to inspire me and keep me moving, as well as the rest of my family, which are too numerous to list here. While Jim Cobble and others in Boy Scout Troop 129 instilled into me the love of the great outdoors, it was faculty members at University of New Mexico who helped me understand the amazing nature that is geology and the geosciences. These faculty members are John Geissman, Karl Karlstrom, Laurie Crossey, Jane Selverstone, and Horton Newsom. My research advisor here at New Mexico Tech, Glenn Spinelli, has been one of the best advisors that I could have hoped for. His patience, teaching ability, and accessibility have been nothing short of amazing. The faculty in the Hydrology department at New Mexico Tech is made up of some of the best people that I have had the pleasure of learning from, and teach an excellent program. My graduate committee, Mark Person of New Mexico Tech and Monty Vesselinov at Los Alamos National Laboratories has been great references for information. Dave Broxton and Rich Morley were invaluable help at Los Alamos National Laboratories. I made many great friends at New Mexico Tech, and will remember this learning experience for the rest of my life. My final thanks go to Clay Kilmer, Bob Newcomer, and others at Golder Associates, who have provided me with the next step to my future in a great career. Los Alamos National Laboratories supported this research.

TABLE OF CONTENTS

LIST OF TABLES

LIST OF FIGURES

INTRODUCTION

The Bandelier Tuff is comprised of a series of ash-flow tuff deposits from the Valles Caldera in the Jemez Mountains, north-central New Mexico. The Bandelier Tuff is widespread over the Jemez Mountains; this study focuses on the portion of the Pajarito Plateau owned by Los Alamos National Laboratory (LANL) (Figure 1). The Pajarito Plateau is located on the east flanks of the Valles Caldera. It is located at the active boundary between the Colarado Plateau and Rio Grande Rift (Broxton and Vaniman 2005).

Residential water supply wells on the Pajarito Plateau draw water from depths of 2000-3110 feet below ground surface (Purtyman 1995), (Koch and Rogers 2003). The water table lies largely in the Puye Formation with water table depths 200-800 feet below the ground surface (Cole, et al. 2009). The Puye Formation is a tertiary-aged sedimentary conglomerate deposited by Rio Grande Rift in-fill as well as riverine deposits from the Rio Grande and ancestral Rio Chama. Past release activity at LANL has resulted in elevated concentrations of tritium, nitrate, high explosives, perchlorate, and other mobile contaminants in shallow and intermediate perched systems in the vadose zone, which are found in the Bandelier Tuff (Newman and Robinson 2005). Perched zones are most commonly encountered at the base of the Bandelier Tuff, lying atop low-permeability Cerros del Rio basalts. Contaminants are mainly contained in the

vadose zone, but there has been a history of low concentrations of contaminants found in the regional aquifer.

Ash-flow tuffs are widely distributed throughout the southwest United States, with few being as well studied as those near Yucca Mountain, southern Nevada, or the Bandelier Tuff. The ash-flow tuffs at Yucca Mountain are over 1000 m thick, completely in the vadose zone. The sequence of tuffs is comprised of beds of rhyolitic lavas and pyroclastic deposits. Theses separate units display a large degree of variation in formation thickness, crystallization, alteration, and welding. Porosity was found to range from 2 to 60 percent (Flint and Selker 2003), while saturated hydraulic conductivity was found in ranges from 1 x 10^{-4} to 1 x 10^{-14} m/s. Data from (Flint and Selker 2003) and (Istok, et al. 1994) were used to create a conceptual model to determine zones of maximum and minimum welding in ash-flow tuffs, as well as saturated hydraulic conductivity and porosity variations.

This study focuses on the correlations between geophysical and hydrologic data in boreholes drilled on LANL property. Geophysical logging data is generally more extensive than hydrologic data for wells on LANL property. Therefore, data available from geophysical logging in the Bandelier Tuff can be a valuable proxy for hydrologic information in the study area.

GEOLOGY/HYDROGEOLOGY

The Bandelier Tuff makes up a significant portion of the vadose zone on the Pajarito Plateau, which is located on the flanks of the Valles Caldera in north-central New Mexico. The Bandelier Tuff is a unit of multiple ash-flow tuffs deposited by massive eruptions from the Valles Caldera. The Bandelier Tuff overlies a sequence of Cerros del Rio Basalts, Puye Formation, the Totavi Lentil, and finally the ancestral Santa Fe Group sediments (Broxton and Vaniman 2005).

This study investigates the deep vadose zone and possible perched zones in the Bandelier Tuff. Perched zones are most commonly found at the base of the Otowi Member of the Bandelier Tuff, atop the less-permeable Cerro del Rio Basalts (Broxton and Vaniman 2005). The boreholes investigated in this study are from canyons deemed "wet" by (Birdsell, et al. 2005). Wet canyons have headwaters in the mountains, large catchment areas, surface flows that frequently occur, and perched alluvial groundwater which exists beneath the canyon floor. Models for wet canyons in Birdsell et al. (2005), suggest a lateral flow to the water in the vadose zone and perched groundwaters.

Ash-Flow Tuff General Characteristics

Ash flow tuffs exhibit heterogeneous physical properties due to spatial variability in cooling rates and compaction (Istok, et al. 1994). Ash flow tuffs are found to be

thickest near the volcanic center (Ross and Smith 1961). The unit thickness decreases with distance from the volcanic center, eventually pinching out (Figure 2).

Significant plastic deformation (welding) in ash flow tuffs is found to be strongest towards the volcanic center. For a vertical cross-section through a tuff deposit, welding is strongest in the central portion of the tuff deposit. Welding is stronger in the inner portion due to the heat trapped in the tuff deposit, as well as compaction from the top of the tuff deposit. Welding decreases porosity and hydraulic conductivity as the tuff recrystallizes and deforms. The upper and lower boundaries of the flow unit are expected to exhibit higher porosity and saturated hydraulic conductivity where cooling occurs much more quickly with interactions with the atmosphere or underlying ground surface. Hydraulic conductivity is found to follow the same trend as porosity. The vertical trends in physical and hydrologic properties are expected to be less apparent at the distil end of the flow. As distance from the volcanic center increases, the welding effects are less pronounced due to the increased heat loss from the thinner unit, as well as a lower degree of compaction.

Geophysical parameters of the ash-flow tuff in dry and wet conditions were measured by (Roberts, Carlberg and Lin 1998). Dry ash-flow tuff samples have resistivities ranging from 10^{-7} to 10^{-8} ohm-m. As fresh water saturation increases, resistivity of the formation drops to 1,000 to 3,000 ohm-m. As fresh water saturation increases to greater than 50%, resistivity of the formation can drop from 100 to 400 ohm-m.

Geologic History of Pajarito Plateau

The Pajarito Plateau is comprised of volcaniclastic and sedimentary rocks reflecting the Miocene through Quaternary tectonism along the western margin of the Española Basin. The Pajarito Plateau overlies the deepest part of the Española Basin and is bounded by the Pajarito Fault on the western margin. The Bandelier Tuff overlies an assemblage of Miocene to Pliocene basin-filling sedimentary and volcanic rocks.

Before the Bandelier Tuff units were deposited, the ancestral Pajarito Plateau was a sedimentary basin being in-filled by Santa Fe Group sediments from the Rio Grande Rift as well as the Puye Formation, ancestral Rio Chama deposits. Cerros del Rio Basalts flowed over the eastern portions of the Pajarito Plateau with some interfingering with the Puye Formation.

The Bandelier Tuff was deposited during large eruptions from the Valles Caldera 1.6 and 1.2 Ma. The 1.6 Ma eruption deposited the Otowi Member of the Bandelier Tuff, which is described as a large, non-welded poorly consolidated unit (Broxton and Vaniman 2005), (Griggs 1964). The Cerro Toledo interval results from a period of sedimentation in between major eruptions (Stix, et al. 1988) (Bailey, Smith and Ross 1969). During this time, the loose unconsolidated sediments in the Otowi member were eroded to form canyons and mesas which give the Pajarito Plateau its distinctive appearance today. The last major eruption of the Valles Caldera deposited the Tshirege Member, made up of multiple surge and cooling beds (Figure 3).

The mineralogy of the ah-flow tuffs is largely comprised of feldspar, volcanic glass, and mafic phenocrysts. Sanadine grains are noted in lower subunits of the Tshirege member. These ash-flow tuffs contain high amounts of Potassium in both primary

feldspars and secondary feldspars albite and adularia (Richard Warren 2005), as well as trace amounts of Uranium-oxide and Thorium-oxide.

Tshirege Member, Qbt

The Tshirege member is the uppermost member of the Bandelier Tuff. It is the most widely exposed bedrock unit, consisting of multiple cooling subunits (Broxton and Vaniman 2005). Of the four noted subunits, this study investigates the lower three. The Tshirege Member was deposited by multiple eruptions from the 1.2 Ma eruption period of the Valles Caldera. The thickness of the Tshirege Member ranges from 61 m in the North-Central part of LANL to 183 m near the southern edge of LANL.

Qbt 3t

The Qbt 3t subunit is described by Broxton and Vaniman (2005) as a moderately to densely welded ash-flow tuff which has lithologic and geochemical characteristics transitional between the Qbt 3 and Qbt 4 members. It is an additional subunit located in the extreme western part of LANL. Qbt 3 is a nonwelded to partly welded tuff which forms the caprock of mesas of the central Pajarito Plateau. Samples from the unit 3t of the Tshirege Member are densely welded is a densely welded of largely gray color. The tuff contains grains of glass and sanadine. Figure 4 shows a representative core sample from Qbt 3t.

Qbt 2

The Qbt 2 tuff is typically the most strongly welded tuff in the Tshirege Member. It forms a distinctive brown-colored vertical cliff forming unit, which is markedly different than the grayer, slope forming subunits above and below. Welding is noted to increase up-section through the subunit (Broxton and Vaniman 2005). It is also reported to have lower porosity and greater density than the surrounding subunits in the Tshirege member. Samples from the unit 2 of the Tshirege Member consist of pale brown, moderately welded devitrified tuff with felsic phenocrysts in a fine ash matrix. Decreased levels of welding in the samples are likely from disturbance during the coring process. Figure 5 shows a representative core sample from Qbt 2.

Qbt 1v

The Qbt 1v subunit forms alternating cliff and slope outcrops composed of porous, non-welded, crystalline tuffs. The 'v' indicates vapor-phase crystallization that along with crystallization of glass in shards and pumices transformed the rock matrix into microcrystalline aggregates of silica polymorphs and sanidine. Samples from Qbt 1v are grayish orange pink to light brown in color. The subunit is a poorly welded devitrified tuff. The texture is pumice-rich with felsic phenocrysts and lithics contained in a fine ash matrix. Figure 6 shows a representative core sample from Qbt 1v.

Qbt 1g

Qbt 1g is the lowermost subunit of the ash-flow tuffs in the Tshirege Member. It contains porous, non-welded, and poorly sorted ash-flow tuffs. The 'g' indicates 'glass';

none of the glass in ash and pumice exhibits crystallization by devitrification or vapor phase alteration. There is a resistant bench near the top of the subunit which forms a cap over the softer underlying tuffs. Samples from Qbt 1g are light brown to grayish orange in color. The poorly welded tuff is composed of felsic crystals and vitric pumice fragments, contained in a fine to coarse vitric ash matrix. Figure 7 shows a representative core sample from Qbt 1g.

Cerro Toldedo Interval, Qct

The Cerro Toledo Interval is stratified sequence of volcaniclastic sediments and some tephra from multiple sources. It uncomformably overlies the Otowi Member. Samples from the Cerro Toledo interval are grayish orange to moderately yellowish brown gravelly sandstone and siltstones, with cobble-sized inclusions of pumice and volcanic gravel. The basal portion of the Cerro Toledo interval is mostly composed of subangular, intermediate volcanic lithics. Figure 8 shows a representative core sample of Qct.

Otowi Member, Qbo

The Otowi Member of the Bandelier Tuff was deposited by the 1.6 Ma eruption event of the Valles Caldera. It is a moderately consolidated, porous, non-welded ash flow tuff that forms colluvium-covered slopes along the base of canyon walls. The Otowi Member is made up of tuffs that are vitric and contain light gray to orange pumice supported in a white to tan ashy matrix of glass shards, broken pumice, crystals, and rock fragments. Like the Tshirege Member, the Otowi Member is made up of individual ash

flows, but the Otowi subunits do not exhibit variability in texture, welding, or density. For this reason, the Otowi member collectively forms a relatively homogenous non welded ash-flow tuff throughout the plateau. Samples from the Otowi Member are dark yellowish orange to grayish orange to very light gray and poorly welded. They contain intermediate composition volcanic and vitric pumice fragments in a fine, vitric ash matrix. Figure 9 shows a representative core sample from Qbo.

METHODOLOGY

Sample locations

Samples were obtained from boreholes through the LANL complex to investigate spatial variability. Samples were then chosen from boreholes with available geophysical data. Core samples were then chosen based on competency and length greater than 0.3 feet.

Site LAOI-3.2 is the furthest borehole from the Jemez Mountain center in this investigation (Fig. 1). It is located in the canyon bottom in Los Alamos Canyon which experienced tremendous erosion, limiting the availability of multiple subunits. Samples were collected from borehole LAOI-3.2 in the Otowi Member, 26.8-147 feet below ground surface (bgs). Samples were obtained in the intervals from 64-65 feet bgs, 134.4-135 bgs, and 136.3-137.3 feet bgs (Kleinfelder 2006) (Figure 10).

Site LADP-5 is located up Los Alamos Canyon in DP canyon, where erosion was less active and more subunits are still in place than in LAOI-3.2 (Fig. 1). Samples were collected from the LADP-5 borehole in Qbo (266.5-494 feet bgs), Qct (237.6-266.5 feet bgs), Qbt 1g (139-237.6 feet bgs), Qbt 1v (67-139 feet bgs), and Qbt 2 (1.3-67 feet bgs). The Otowi member was sampled at 276.4-277.4 feet bgs and 280-280.8 feet bgs (Kleinfelder, Inc. 2006). The Cerro Toledo interval was sampled at 244-245 feet bgs. The Tshirege 1g member was sampled at 194-195 feet bgs. The Tshirege member 1v

was sampled at 101.3-102 feet bgs. The Tshirege 2 member was sampled at 54-55 feet bgs (Figure 10).

Site PCI-2 was cored at the bottom of Pajarito Canyon (Fig. 1). Erosion has been less active in Pajarito Canyon, allowing samples further up in the Tshirege cooling units. Samples were collected from the PCI-2 borehole in the Tshirege 1g member (33-131 feet bgs) and the Cerro Toledo interval (131-156 feet bgs). Four samples were obtained from the Tshirege 1g member from 47-47.5 feet bgs, 57-58 feet bgs, 62-62.5 feet bgs, and 129 – 130 feet bgs. One sample was obtained from the Cerro Toledo interval from 135-136.5 feet bgs (Figure 10).

Site R-25 is the closest borehole to the Jemez Mountain center. Erosion has been limited at this site; most subunits are well preserved at this site. Samples were collected from the R-25 borehole in Qbt 3t (84-155 feet bgs), Qbt 2 (228-332 feet bgs), Qbt 1v (332-369 feet bgs), Qbt 1g (369-384 feet bgs), Qct (384-740 feet bgs). The Qbt 3t subunit was sampled at 92.2-92.5 feet bgs. The Qbt 2 subunit was sampled at 246-246.5 feet bgs. The Qbt 1v subunit was sampled at 359.7-360.2 feet bgs. The Qbt 1g subunit was sampled at 372.5-373 bgs. Qct was sampled at 566-566.5 feet bgs (Figure 10).

Saturated hydraulic conductivity falling-head tests

Saturated hydraulic conductivity (K) was measured using a falling-head method (Freeze and Cherry 1979). Core samples were pre-packed into Lexan tubing with a tight fit in between the tubing and the core wall. Sediment retention plates were placed over the ends of the Lexan core sleeves, and then caps with a barb tube outlet. Time was

measured as the head of de-aerated water fell from the initial height to the final height, and saturated hydraulic conductivity was computed using Darcy's law.

$$K = \frac{aL}{At} \ln \frac{H0}{H1}$$

K – saturated hydraulic conductivity

a – cross-sectional area of tube

A – cross-sectional area of core sample

t – time for head to drop from H_0 to H_1

H_0 – Initial head

H_1 – final head

Porosity tests

Samples were obtained from unconsolidated and friable core into sediment cups. De-aerated water was injected into the bottom of the sample cup, completely saturating the porosity in the sample with water. Porosity was then calculated by comparing wet and dry mass for a known volume of sample. Samples from strongly welded units could not be removed from the core and were measured inside of their supplied core tubing.

Degree of welding

The degree of welding in samples was determined by measuring the aspect ratios of fiamme (collapsed pumice inclusions) in the samples. More heavily welded samples

have horizontally long, vertically thin fiamme, with aspect ratios up to 4.5:1, while faimme in poorly welded samples have a roughly 1:1 aspect ratio. Multiple fiamme were measured in each sample with the core in an upright position, and final result was averaged to a single aspect ratio.

Geophysical logging data collection and analysis

Geophysical logging measurements were obtained through the use of a LANL-owned Mount Sopris geophysical logging array, which is used to record natural gamma and induction data. Natural gamma and resistivity logs were run with the LANL geophysics trailer in the LADP-5, LAIO-3.2, R-25, and PCI-2 (Kleinfelder, Inc. 2006) boreholes. Boreholes LAOI-3.2, LADP-5, and PCI-2 data were logged in open holes with no steel casing. Borehole R-25 data were logged with 12" casing over the entire depth. Calibration corrections were performed where needed (Figure 11).

Resistivity logs are measured by using a single downhole current electrode which emits an electric signal into the rock and multiple downhole potential electrodes to record resistivity measurements at different electrical spacing distances. In these analyses, the 20" spacing was measured for analysis. Resistivity is calculated using Archie's empirical formula (Johnson Screens 2007):

$$r_e = a\eta^{-m}S^{-n}r_w$$

r_e - resistivity of formation at 100% saturation

η – porosity

S – saturation: fraction of pores containing water

r_w - resistivity of water

a, n, m – constants

0.5 ≤ a ≤ 2.5

1.3 ≤ m ≤ 2.5

Assuming all other values remain constant, a decrease in porosity will increase the resistivity of the formation at 100% saturation.   This is due to the increased interconnectivity of the rock unit.   Using the same assumption, a decrease of the saturation, or number of pores that contain water, will also increase the resistivity of the formation at 100% saturation.

Gamma-ray data were analyzed in this study.   However, the data provides no spatial trends because of the naturally high levels of potassium and thorium in ash-flow tuffs. Gamma-ray values are high due to the high concentrations of radiogenic potassium and thorium. However, the gamma-ray logs are useful for determining subunit contacts in the field.

RESULTS

Geophysical Data

Gamma-ray values are useful in this study to mark unit contacts. Due to the high concentrations of radiogenic elements (K, Th, U) and minerals (feldspar) in the ash-flow tuff, the gamma-ray values are only useful as a marker for subunits (Table 1). The gamma-ray values are similar with distance from the Jemez Volcanic center. The later tuff subunits deposited higher on the pile have a lower gamma ray count. Qbt 1v and Qbt 1g have a very similar gamma ray count, which decreases in Qct. Qbo has a relatively low gamma-ray count (Figure 5).

Gamma-ray values in Qbt 3t are relatively low at 170.3 API. Gamma-ray values for Qbt 2 are 199.2 API at R-25 to 190.0 API at LADP-5. Gamma-ray values for Qbt 1v range from 191.8 API in PCI-2 to 266.7 API at R-25. Higher gamma-ray values are in the center of the Qbt 1g subunit in PCI-2, and lower gamma-ray values are near the top and bottom of the unit (Figure 5c).

Gamma-ray values for Qct are relatively low and similar, around 180 API. Gamma-ray values for Qbo are most commonly lower than those found the Tshirege subunits, but they also display a large variability. Both the lowest and highest gamma-ray values in this study are in the Qbo subunit. Gamma-ray values range from 132.9 API in R-15 to 277.1 API at the upper sampling point in LAOI-3.2.

Resistivity is found to decrease with distance from the Jemez Mountain center. Resisitivities are higher in the middle units of the Tshirege Member (Qbt 2, Qbt 1v, Qbt 1g) (Table 2, Figure 12). The resistivity is relatively low in subunit Qbt 3t at the R-25 borehole. The resistivity is 178.8 ohm-m. The resistivity for R-25 is much higher in the Qbt 2 subunit at 200.3 ohm-m. Further from the Jemez Volcanic center at LADP-5, the resistivity is 225.7 ohm-m. The resistivity in the Qbt 1v subunit is also much higher at R-25, near the Pajarito Fault, that LADP-5. At R-25, the Qbt 1v subunit has a resistivity of 370.2 ohm-m, and at LADP-5, the subunit has a resistivity of 181.2 ohm-m (Fig. 13).

The resistivity for Qbt 1g has a high degree of variability. Values in PCI-2 vary from 470.4 to 171.5 ohm-m. Both R-25 and LADP-5 have similar values of 232.5 and 233.6, respectively.

The resistivity of the Cerro Toledo interval exhibits the same behavior as other subunits with higher values hear the pajarito Fault. R-25 has a resistivity of 241.0 ohm-m, PCI-2 has a resistivity of 70.3 ohm-m, and LADP-5 has a resistivity of 100.3 ohm-m.

The resistivity of Qbo also displays some high variability in a small spatial range. LADP-5 has resistivity values of 319.5 and 290.1 ohm-m in the upper portion of the subunit, while LAOI-3.2 has resistivity values of 122.0 to 65.4 ohm-m, with the lowest values being near the bottom of the subunit.

Saturated hydraulic conductivity

Saturated hydraulic conductivity ranges from 7.82×10^{-6} to 1.52×10^{-3} cm/sec. Higher hydraulic conductivity values (up to two orders of magnitude) are found closer to

the Jemez Mountain center, and lower values are found at greater distances from the source caldera. Overall, most caprock units exhibit lower hydraulic conductivities than the underlying ash-flow tuffs (Figure 15, Table 3).

Qbt 3t is found only near the Pajarito fault at borehole R-25. It marks the lowest hydraulic conductivity for R-25 at 7.82×10^{-4} cm/sec.

Qbt 2 is found extensive throughout the mesa tops and the upper reaches of canyons across the LANL complex. Hydraulic conductivity values decrease from 2.11×10^{-3} cm/sec at R-25 to 7.82×10^{-6} cm/sec at LADP-5.

Qbt 1v is also found extensively through the LANL complex. Hydraulic conductivity values decrease from 1.52×10^{-3} cm/sec at R-25 to 2.62×10^{-5} cm/sec at LADP-5.

Qbt 1g was sampled a multiple depths in the PCI-2 borehole. The hydraulic conductivity values range from 4.15×10^{-3} cm/sec at R-25 to 3.09×10^{-5} at LADP-5. The four samples from the PCI-2 borehole range from 1.63×10^{-4} cm/sec to 4.54×10^{-5} cm/sec.

Qct has a hydraulic conductivity range of 2.74×10^{-3} cm/sec at PCI-2 to 9.10×10^{-5} cm/sec at LADP-5. The hydraulic conductivity of Qct at the R-25 borehole is actually less than that of PCI-2 at 4.56×10^{-3} cm/sec.

Qbo was the most widely sampled unit. The R-25 borehole did not reach the depth to obtain samples from Qbo. The hydraulic conductivity values vary from 1.86×10^{-5} cm/sec at LAOI-3.2 to 8.73×10^{-5} cm/sec at LADP-5.

Porosity

Porosity is highly variable, ranging from 26.3% to 43.3% (Figure 13, Table 2). Qbt 2 has a porosity of 40.3% at LADP-5.Qbt 1v has a porosity of 34.7% at R-25 and 43.3% at LADP-5.

Qbt 1g has a porosity ranging from 30.3% to 43.3% in boreholePCI-2. On a spatial scale, there is a porosity of 31.2% at R-25 and 38.4% at LADP-5. The downward trend of porosity at PCI-2 is not in accordance with the model presented by Istok et al (1994).

Qct has a porosity ranging from 29.5% at LADP-5 to 39.3% at PCI-2. The porosity at R-25 is close to that of LADP-5 at 30.3%. Qbo has a porosity range from 26.3% at R-15 to 42.3 % at LAOI-3.2. Porosity tends to be higher in the boreholes from Los Alamos and DP canyons compared to those in Mortandad canyon.

Degree of Welding

The welding of the tuff units ranges from 4.5:1 to 0.69:1 horizontal–to-vertical aspect ratios of fiamme in ash-flow tuff core samples. The greater aspect ratios correlate with ash-flow tuffs with a greater degree of welding. Lesser aspect ratios, especially those that are less than 1:1 correlate with poorly to non-welded tuffs.

Strongly welded to welded fiamme samples from Qbt 3t and Qbt 2 subunits have the greatest aspect ratios. Fiamme in Qbt 3t have an aspect ratio of 4.50:1. Samples from Qbt 2 have the next highest aspect ratios, 1.83:1 at R-25 and 2.55:1 at LADP-5.

Poorly welded samples from Qbt 1v have aspect ratios of 1.43:1 at R-25 and 1.29:1 at LADP-5. Samples for Qbt 1g are also poorly welded, but average a higher

degree of welding than the overlying Qbt 1v unit. The aspect ratios range from 1.71:1 at R-25 to 1.38:1 at LADP-5. Samples of Qbt 1g in PCI-2 have a slightly higher aspect ratio than the others in Qbt 1g, ranging from 1.50:1 to 1.83:1.

The non-welded samples of Qbo have extremely low aspect ratios, ranging from 0.69:1 to 1.12:1. Fiamme from LAOI-3.2 have aspect ratios of 0.85:1 to 1.12:1, while fiamme from LADP-5 range from 0.69:1 to 0.92:1. The pumice clasts are relatively rounded, suggesting no compression due to heat or overburden, and thus no welding.

Correlative Trends

There are two strong trends in the data, and they represent changes of both hydrologic and geophysical properties with relation to distance from the source Jemez Volcanic Center. Both saturated hydraulic conductivity and resistivity decrease with distance from the Jemez Volcanic center (Tables 1 & 4, Figures 13 & 15).

There are few trends in between the geophysical data and hydrologic data. Porosity has a poor correlation with both resistivity and saturated hydraulic conductivity.

DISCUSSION/INTERPRETATION

The Bandelier Tuff exhibits parameters that are well-defined by previous research on ash-flow tuffs. In a typical ash-flow tuff, both hydraulic conductivity and porosity are higher at the top and bottom of the subunit, and lower towards the middle from welding due to intrinsic heat and overburden compression (Ross and Smith 1961). The effect is found to be less pronounced with increasing distance from the volcanic source.

There is no significant decrease in porosity with distance from the Jemez Volcanic Center. However, saturated hydraulic conductivity decreases with distance from the volcanic source. Possible explanations for deviations from the model presented by Istok et al. (1994) include: 1) The rapid deposition of successive subunits may have affected the cooling rate, and therefore the degree of welding, and 2) relatively small deposits for each subunit reduces overburden weight and time of high temperature for welding.

The degree of welding in ash-flow tuff subunits is strongest in units designated heavily welded (Qbt 3t & Qbt 2), and lesser to non-existent in units designated poorly to non-welded (Qbt 1v, Qbt 1g, Qbo). The degree of welding follows the lateral trend described by (Istok, et al. 1994), where the degree of welding decreases with distance from the source caldera. Deviations from model behavior can be attributed to local zones of pre-existing topography, where more of the subunit was able to accumulate as the cooling and welding began, increasing overburden pressure and heat, thus increasing the degree of welding.

Geophysical logging of these extensive ash-flow tuffs provides data useful for identifying contacts between subunits in the Bandelier Tuff. However, high potassium and thorium contents of the minerals in the Bandelier Tuff subunits make the data useful as a marker between the contacts of subunits.

The trend in resistivity can be described by the lateral flow of water in the deep vadose zone of wet canyons (Birdsell, et al. 2005) and the increasing mineralization of water as it moves through the vadose zone system. Another explanation lies in the relationship between the degree of welding and the resistivity. As the degree of welding decreases, the connectivity of the grains in the ash-flow tuff decreases. The lesser connectivity of the tuffs results in a lesser resistivity value.

CONCLUSION

This study focused on the Bandelier Tuff portion of the vadose zone beneath LANL. The multiple subunit depositions in the Tshirege Member subunits changed the cooling pattern, and thus the welding of the subunit. These changes in welding create atypical patterns through the subunits for porosity and hydraulic conductivity. The variability in welding, density, and porosity noted in between the subunits is driven by time in between eruptions, where the recently placed ash flow tuffs had differing cooling and welding times before the next subunit was deposited.

Hydrologic parameters change with distance from the Jemez Volcanic Center. Following the model from (Istok, et al. 1994), the saturated hydraulic conductivity decreases with distance from the source caldera due to a thinner deposition of ash-flow tuff, which cools more quickly and welding is less pronounced than in the thicker depositions closer to the caldera. Local variations are due to existing topography prior to deposition, creating deeper pockets further from the source caldera which can create local zones of higher degree of welding. The change in saturated hydraulic conductivity correlates with the degree of welding, which also decreases with distance. Porosity varies more greatly than the hydraulic conductivity, but the porosity does decrease with distance from the caldera. The porosity values in the Tshirege Member of the Bandelier Tuff do not follow the models set forth by (Istok, et al. 1994) and (Flint and Selker 2003) possibly due to the rapid deposition of multiple subunits. In this scenario, the separate

cooling units did not have time to fully cool and weld before the deposition of the next subunit.

Additional work on this project can be used to improve the relationships between resistivity and saturated hydraulic conductivity. To further constrain the mineral content of the water, which affects resistivity, groundwater residence times can be calculated. This effect may also obtained by measuring TDS in groundwater samples from perched or highly saturated zones. Additional geophysical logs, such as neutron and spontaneous potential, can be investigated for further information. Spontaneous potential logs are helpful for determining water-saturated zones. Neutron logs are useful for calculating porosity, which can be used as a comparison to porosity measured in the lab.

Geophysical parameters change with distance from the Jemez Volcanic center. The resistivity values decrease with distance from the caldera. This relationship can be explained by the lateral flow of water in the vadose zone of wet canyons (Birdsell, et al. 2005) interacting with the ash-flow tuff material and absorbing the minerals, thus decreasing the resistivity. Gamma-ray values remain fairly constant throughout the subunits due to the high amount of naturally-occurring potassium and thorium in the ash-flow tuff materials. The distinct changes in gamma ray values aid in defining subunit contacts, as well as resistivity values.

REFFERENCES

Bailey, R. A., R. L. Smith, and C. S. Ross. "Stratigraphic Nomenclature of Volcanic Rocks in the Jemez Mountains, New Mexico." (U. S. Government Pringing Office) 1969: P1-P19.

Birdsell, Kay H., Brent D. Newman, David E. Broxton, and Bruce A. Robinson. "Conceptual MOdels of Vadose Zone Flow and Transport beneat the Pajarito Plateau, Los Alamos, New Mexico." *Vados Zone Journal* 4 (2005): 620-636.

Broxton, D. E., and D. T. Vaniman. "Geologic Framework of a Groundwater System on the Margin of a Rift Basin, Pajarito Plateau, North-Central New Mexico." *Vadose Zone Journal* 4 (2005): 522-550.

Cole, G, D Broxton, D Koning, and V Vesselinon. *2009 Hydrogeologic Site Atlas.* Los Alamos, New Mexico : Los Alamos National Security, LLC, 2009.

Flint, Lorraine E, and John D Selker. "Use of porsity to estimate hydraulic propertiesof volcanic tuffs." *Advances in Water Resources* 26 (2003): 561-571.

Freeze, R. A., and J. A. Cherry. *Groundwater.* NJ: Prentice-Hall, 1979.

Griggs, R. L. *Geology and Ground-Water Resources of the Los Alamos Area New Mexico.* Washington, D.C.: United States Government Printing Office, 1964.

Istok, J. D., C. A. Rautman, L. E. Flint, and A.L. Flint. "Spatial Variability in Hydrologic Porperties of a Volcanic Tuff." *Groundwater* 32, no. 5 (1994): 751-760.

Johnson Screens. *Groudwater and Wells.* Edited by Robert J. Sterrett. new Brighton, MN: Litho Tech, 2007.

Kleinfelder, Inc. *Final Completion Report Intermedate wells LAOI-3.2 and LAOI-3.2a Los Alamos Nataional Laboratory.* Albuquerque, New Mexico: Kleinfelder, Inc., 2006.

Kleinfelder, Inc. *Final Completion Report Intermediate Well LADP-5 Los Alamos National Laboratory Los Alamos New Mexico.* 12, Albuquerque, New Mexico: Kleinfelder, Inc., 2006.

Koch, R. J., and D. B. Rogers. "Water Supply at Los Alamos, 1998-2001." (Los Alamos Natl. Lab.) LA-13985-PR (2003).

Newman, Brent D, and Bruce A Robinson. "The Hydrogeology of Los Alamos National Laboratory: Site History and Overview of Vadoes Zone and Groundwater Issues." *Vadose Zone Journal* 4 (2005): 614-619.

Purtyman, W. D. "Geologic and hydrologic records of observation wells, test holes, test wells, supply wells, springs, and surface water stations in the Los Alamos area." (Los Alamos Natl. Lab) LA-12883-MS (1995).

Richard Warren, Fraser Goff, Emily Kluk, James Budahn. "Petrography, Chemistry, and Mineral Compositions for Subunits of the Tshirege Member, Bandelier Tuff within the Valles Caldera and Pajarito Plateau." *Geology of the Jemez Region II*, 2005: 316-332.

Roberts, J.J., E. Carlberg, and W. Lin. *Electrical Properties of Tuff from the ESF as a Function of Water Saturation and Temperature.* Livermore, CA: University of California, 1998.

Ross, Clarence S, and Robert L Smith. *Ash-Flow tuffs: Their Origin, Geologic Relations, and Identification.* Vol. USGS Professional Paper 366. Washington, D.C.: United States Government Printing Office, 1961.

Stix, John, Fraser Goff, Michael P Gorton, Grant Heiken, and Sammy R Garcia. "Restoration of Compositional Zonation in the Bandelier Silicic Magma Chamber Between Two Caldera-Forming Eruptions: Geochemistry and Origin of the Cerro Toledo Rhyolite, Jemez Mountains, New Mexico." *Journal of geophysical Research* 93, no. B6 (1988): 6129-6147.

Table 1: Porosity measurements & results

Corehole	Sample depth	Geologic Unit	Area of tube	Area of Core	Length of Core	Initial head	Final head	time	Saturated Hydraulic conductivity
			a (cm^2)	A (cm^2)	L (cm)	Ho (cm)	H1 (cm)	t (sec)	K (cm/sec)
	(ft)								
LADP-5	54-55	Qbt 2	0.2	38.3	30.5	54	39	2880	7.82E-06
LADP-5	101.3-102	Qbt 1v	0.2	4.9	20.3	65	50	3600	2.62E-05
LADP-5	194-195	Qbt 1g	0.2	38.3	30.5	40	10	3099	3.09E-05
LADP-5	244-245	Qct	0.2	38.3	30.5	53	33	3600	9.10E-06
LADP-5	276.4-277.4	Qbo	0.2	38.3	30.5	51	16.5	3173	2.46E-05
LADP-5	280-280.8	Qbo	0.2	38.3	22.8	54	14	800	8.73E-05
R-25	92.2-92.5	Qbt 3t	0.2	56.7	15.2	63	23	30	7.82E-04
R-25	246-246.5	Qbt 2	0.2	56.7	15.2	90	50	6.5	2.11E-03
R-25	359.7-360.2	Qbt 1v	0.2	56.7	15.2	90	50	9	1.52E-03
R-25	372.5-373	Qbt 1g	0.2	56.7	15.2	90	50	3.3	4.15E-03
R-25	566-566.5	Qct	0.2	56.7	15.2	90	50	3	4.56E-03
LAOI-3.2	64-65	Qbo	0.2	38.3	30.5	50	10	2923	3.81E-05
LAOI-3.2	134.4-135	Qbo	0.2	38.3	18.3	62	22	1628	2.64E-05
LAOI-3.2	136.3-137.3	Qbo	0.2	38.3	30.5	54	20.5	3600	1.86E-05
PCI-2	47-47.5	Qbt 1g	0.2	56.7	15.2	90	50	84	1.63E-04
PCI-2	57-58	Qbt 1g	0.2	56.7	30.5	90	50	605	4.54E-05
PCI-2	62-62.5	Qbt 1g	0.2	56.7	15.2	90	50	19.3	7.09E-04
PCI-2	129-130	Qbt 1g	0.2	56.7	30.5	51	11	1127	6.36E-05
PCI-2	135-136.5	Qct	0.2	56.7	15.2	90	50	5	2.74E-03

Table 2: Saturated hydraulic conductivity measurements and results

Core hole	Sample depth	Geologic Unit	Empty Cup weight	Saturated core cup	Dried core & cup	Total volume	Mass of water removed	Volume of water removed	Volume of solids	Mass of Solids	Porosity
	(ft)		(g)	(g)	(g)	(cm^3)	(g)	(cm^3)	(cm^3)	(g)	(%)
LAD P-5	54-55	Qbt 2	2.4	19.1	13.3	20.2	5.8	5.8	14.4	10.9	40.3
LAD P-5	101.3-102	Qbt 1v	2.2	18	11.9	20.2	6.1	6.1	14.1	9.7	43.3
LAD P-5	194-195	Qbt 1g	2.1	16.2	10.6	20.2	5.6	5.6	14.6	8.5	38.4
LAD P-5	244-245	Qct	2.2	17.8	13.2	20.2	4.6	4.6	15.6	11	29.5
LAD P-5	276.4-277.4	Qbo	2.2	16.2	11.7	20.2	4.5	4.5	15.7	9.5	28.7
LAD P-5	280-280.8	Qbo	2.1	16.1	10.9	20.2	5.2	5.2	15	8.8	34.7
R-25	92.2-92.5	Qbt 3t	359.4	2349.9	2324.4	1113.3045	25.5	25.5	1087.8045	1965	2.3
R-25	246-246.5	Qbt 2	246.2	1589.1	1496.8	636.174	92.3	92.3	543.874	1250.6	17.0
R-25	359.7-360.2	Qbt 1v	2.3	19.4	14.2	20.2	5.2	5.2	15	11.9	34.7
R-25	372.5-373	Qbt 1g	2.2	17.7	12.9	20.2	4.8	4.8	15.4	10.7	31.2
R-25	566-566.5	Qct	2.3	18.6	13.9	20.2	4.7	4.7	15.5	11.6	30.3
LAOI-3.2	64-65	Qbo	2.2	20.2	14.7	20.2	5.5	5.5	14.7	12.5	37.4
LAOI	134.	Qbo	2.4	18	13.	20.2	4.9	4.9	15.3	10.	32.0

-3.2	4-135				1					7	
LAOI-3.2	136.3-137.3	Qbo	2.2	18.5	12.5	20.2	6	6	14.2	10.3	42.3
PCI-2	47-47.5	Qbt1g	2.4	17.3	11.2	20.2	6.1	6.1	14.1	8.8	43.3
PCI-2	57-58	Qbt1g	2.4	16	10.8	20.2	5.2	5.2	15	8.4	34.7
PCI-2	62-62.5	Qbt1g	2.2	18.1	12.6	20.2	5.5	5.5	14.7	10.4	37.4
PCI-2	129-130	Qbt1g	2.3	20	15.3	20.2	4.7	4.7	15.5	13	30.3
PCI-2	135-136.5	Qct	2.2	20.3	14.6	20.2	5.7	5.7	14.5	12.4	39.3

Table 3: Degree of welding measurements and results

Borehole	Depth Start	Depth End	Geologic Unit	Fiamme #1			Faimme #2			avg. aspect ratio
	(ft bgs)	(ft bgs)	(ft bgs)	hor. (ft)	vert. (ft)	aspect ratio	hor. (ft)	vert. (ft)	aspect ratio	
LADP-5	54	55	Qbt 2	0.07	0.02	3.50	0.04	0.025	1.60	**2.55**
LADP-5	101.3	102	Qbt 1v	0.04	0.03	1.33	0.05	0.04	1.25	**1.29**
LADP-5	194	195	Qbt 1g	0.04	0.03	1.33	0.05	0.035	1.43	**1.38**
LADP-5	276.4	277.4	Qbo	0.025	0.035	0.71	0.02	0.03	0.67	**0.69**
LADP-5	280	280.8	Qbo	0.07	0.06	1.17	0.02	0.03	0.67	**0.92**
LAIO-3.2	64	65	Qbo	0.07	0.1	0.70	0.06	0.06	1.00	**0.85**
LAOI-3.2	134.4	135	Qbo	0.1	0.09	1.11	0.03	0.03	1.00	**1.06**
LAOI-3.2	136.3	137.3	Qbo	0.04	0.03	1.33	0.09	0.1	0.90	**1.12**
PCI-2	47	47.5	Qbt 1g	0.05	0.03	1.67	0.04	0.02	2.00	**1.83**
PCI-2	57	58	Qbt 1g	0.03	0.02	1.50	0.03	0.02	1.50	**1.50**
PCI-2	62	62.5	Qbt 1g	0.06	0.035	1.71	0.06	0.035	1.71	**1.71**
PCI-2	129	130	Qbt 1g	0.05	0.03	1.67	0.05	0.03	1.67	**1.67**
R-25	92.2	92.5	Qbt 3t	0.25	0.05	5.00	0.12	0.03	4.00	**4.50**
R-25	246	246.5	Qbt 2	0.12	0.06	2.00	0.1	0.06	1.67	**1.83**
R-25	359.7	360.2	Qbt 1v	0.05	0.03	1.67	0.06	0.05	1.20	**1.43**
R-25	372.5	373	Qbt 1g	0.035	0.02	1.75	0.05	0.03	1.67	**1.71**

Table 4: Geophysical data compared with distance from the Pajarito Fault

Borehole	Depth Start (ft bgs)	Depth End (ft bgs)	Geologic Unit	Distance from Pajarito Fault (feet)	Avg. Gamma (API)	Resistivity (ohm-m)
R-25	92.2	92.5	Qbt 3t	5969	170.313	178.802
LADP-5	54	55	Qbt 2	21808	189.946	225.732
R-25	246	246.5	Qbt 2	5969	199.219	300.282
LADP-5	101.3	102	Qbt 1v	21808	245.123	181.223
R-25	359.7	360.2	Qbt 1v	5969	230.234	370.236
LADP-5	194	195	Qbt 1g	21808	249.169	233.594
PCI-2	47	47.5	Qbt 1g	18365	191.781	
PCI-2	57	58	Qbt 1g	18365	243.845	
PCI-2	62	62.5	Qbt 1g	18365	236.479	470.398
PCI-2	129	130	Qbt 1g	18365	205.266	171.491
R-25	372.5	373	Qbt 1g	5969	266.729	232.519
LADP-5	244	245	Qct	21808	182.222	100.332
PCI-2	135	136.5	Qct	18365	164.836	70.309
R-25	566	566.5	Qct	5969	184.215	241.034
LADP-5	276.4	277.4	Qbo	21808	191.168	319.459
LADP-5	280	280.8	Qbo	21808	193.74	290.102
LAIO-3.2	64	65	Qbo	25273	277.074	121.992
LAOI-3.2	134.4	135	Qbo	25273	189.112	66.852
LAOI-3.2	136.3	137.3	Qbo	25273	204.602	65.397

Table 5: Hydrologic Data compared with distance from Pajarito fault

Borehole	Depth Start (ft bgs)	Depth End (ft bgs)	Geologic Unit (ft bgs)	Distance from Pajarito Fault ft	Ksat cm/sec	Porosity %
LADP-5	194	195	Qbt 1g	21808	3.09E-05	38.4
PCI-2	47	47.5	Qbt 1g	18365	1.63E-04	43.3
PCI-2	57	58	Qbt 1g	18365	4.54E-05	34.7
PCI-2	62	62.5	Qbt 1g	18365	7.09E-04	37.4
PCI-2	129	130	Qbt 1g	18365	6.36E-05	30.3
R-25	372.5	373	Qbt 1g	5969	4.15E-03	31.2

Qct

Borehole	Depth Start (ft bgs)	Depth End (ft bgs)	Geologic Unit (ft bgs)	Distance from Pajarito Fault ft	Ksat cm/sec	Porosity %
LADP-5	244	245	Qct	21808	9.10E-05	29.5
PCI-2	135	136.5	Qct	18365	2.74E-03	39.3
R-25	566	566.5	Qct	5969	4.56E-03	30.3

Qbo

Borehole	Depth Start (ft bgs)	Depth End (ft bgs)	Geologic Unit (ft bgs)	Distance from Pajarito Fault ft	Ksat cm/sec	Porosity %
LADP-5	276.4	277.4	Qbo	21808	2.46E-05	28.7
LADP-5	280	280.8	Qbo	21808	8.73E-05	34.7
LAIO-3.2	64	65	Qbo	25273	3.81E-05	37.4
LAOI-3.2	134.4	135	Qbo	25273	2.64E-05	32
LAOI-3.2	136.3	137.3	Qbo	25273	1.86E-05	42.3

Figure 1: Site Map of LANL and sample boreholes
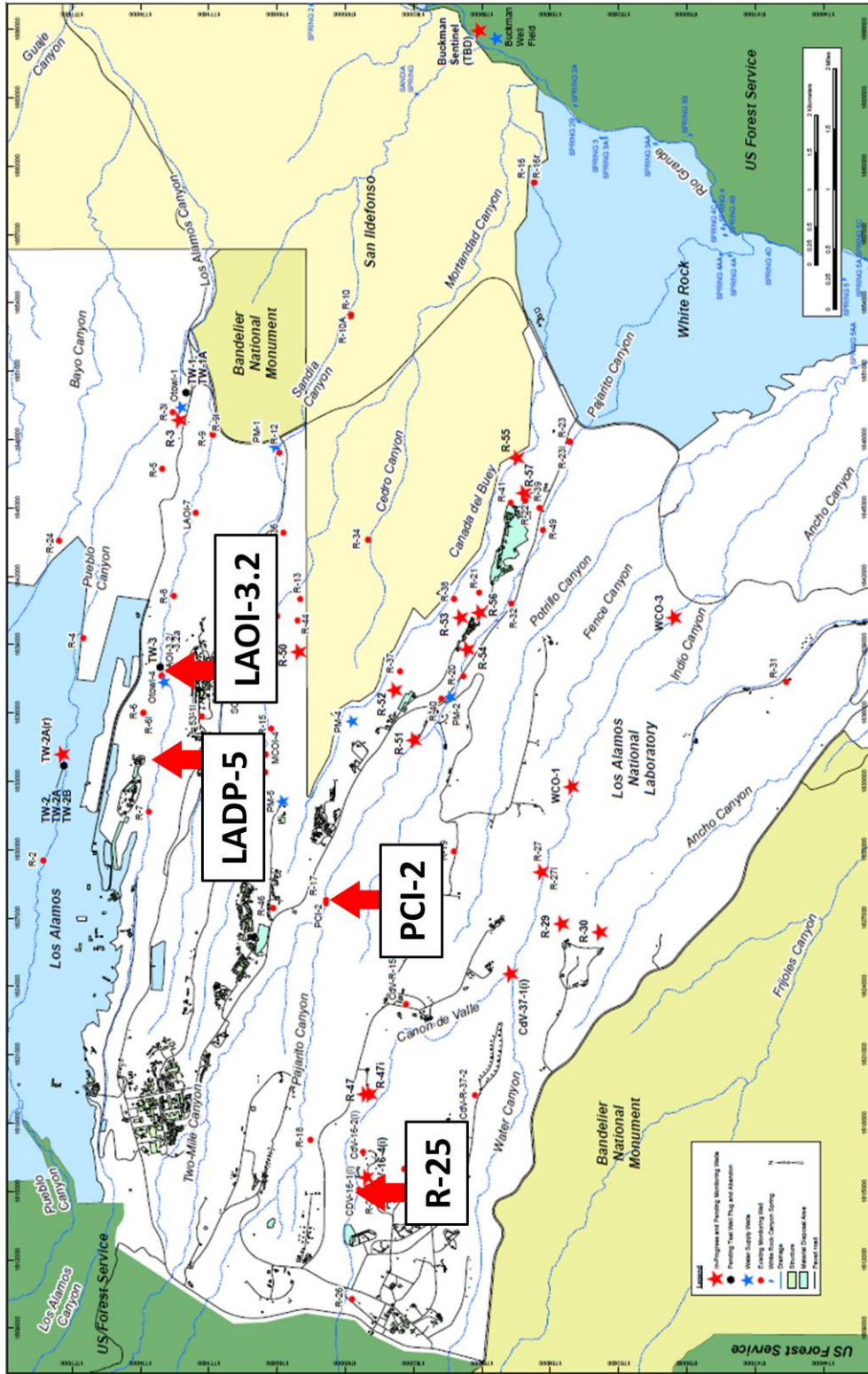
Figure 2: Conceptual model of ash-flow tuff welding zones, exhibiting varying porosity through the section. Modified from (Istok, et al. 1994)
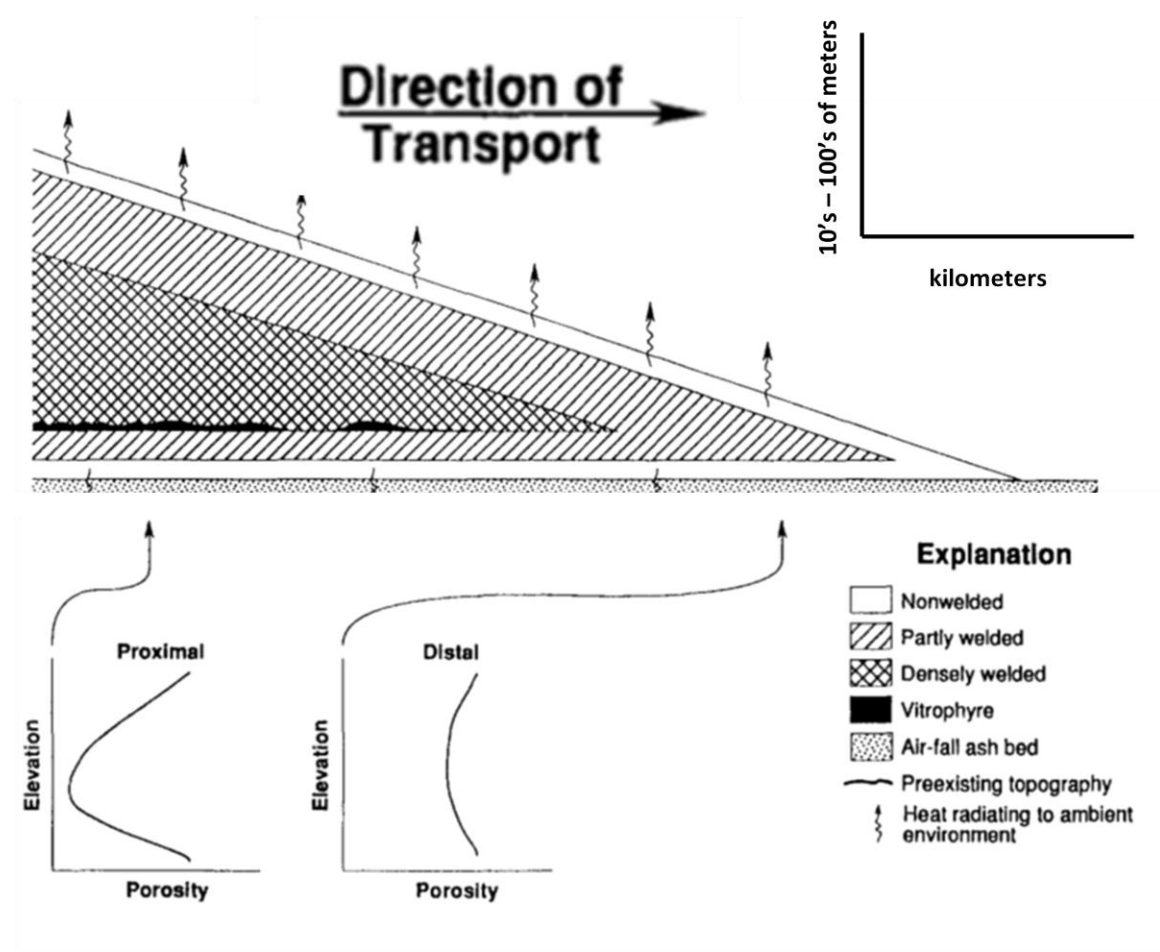
Figure 3: General Stratigraphy of the Bandelier Tuff in the LANL complex

Unit Description

Qbt 3t: Moderate to densely welded, largely gray color

Qbt 2: Strongly welded, brown color

Qbt 1v: Non-welded, grayish orange to light brown color

Qbt 1g: Non-welded, light brown to Gray color

Qct: Sedimentary interval of volcaniclastic material deposited between major eruptions

Qbo: Non-welded, Orange to Gray color
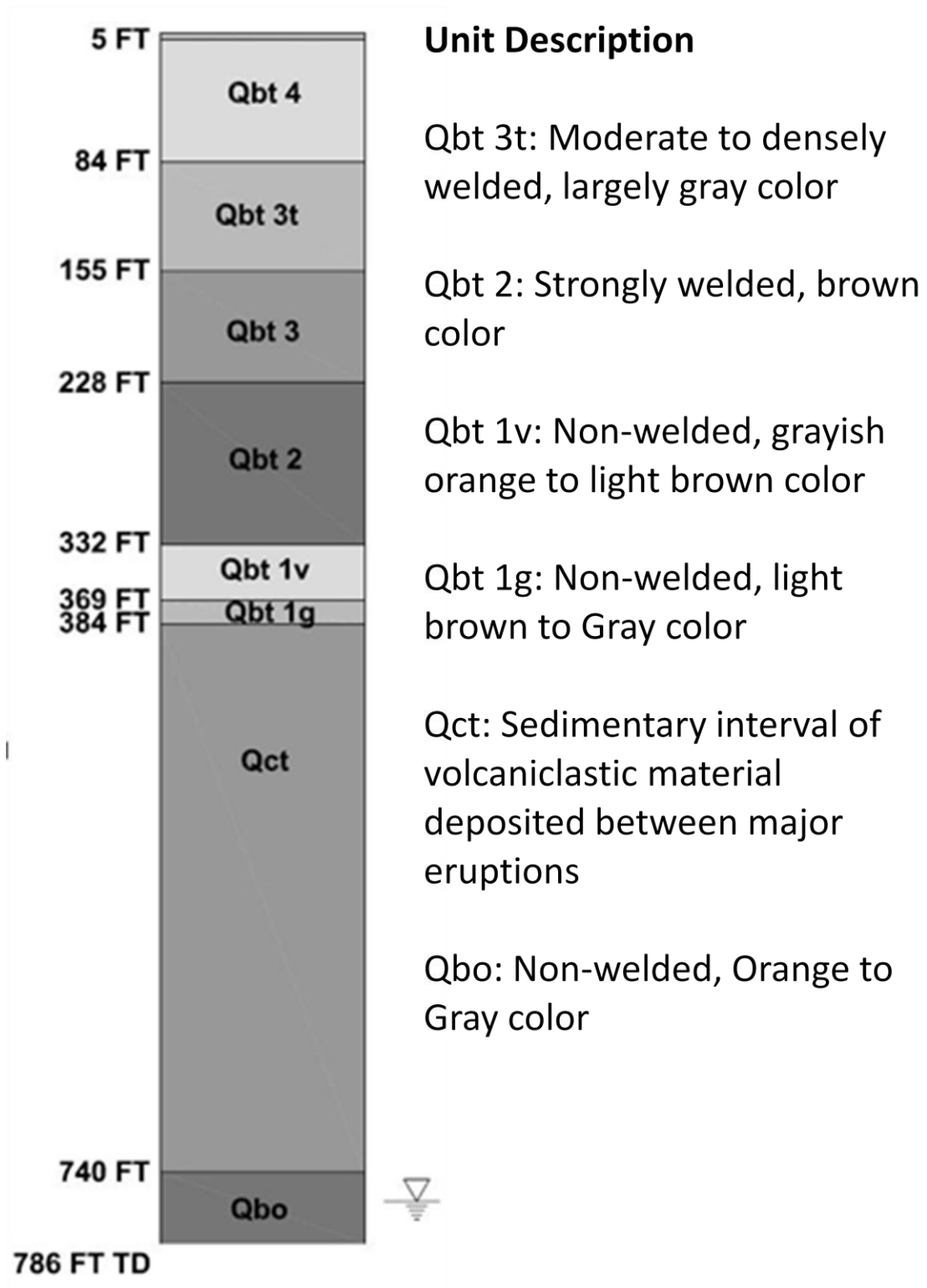
Figure 4: Representative core sample of Qbt 3t from borehole R-25.

Figure 5: Representative core sample of Qbt 2 from borehole LADP-5.

Figure 6: representative core sample of Qbt 1v from borehole LADP-5.

Figure 7: Representative core sample from Qbt 1g from borehole PCI-2.

Figure 8: Representative core sample of Qct from borehole LADP-5.

Figure 9: Representative core sample from Qbo from borehole LAOI-3.2.

Figure 10: Stratigraphic columns from each sample borehole with arrows marking sample locations. Scale bar on left is depth (feet).
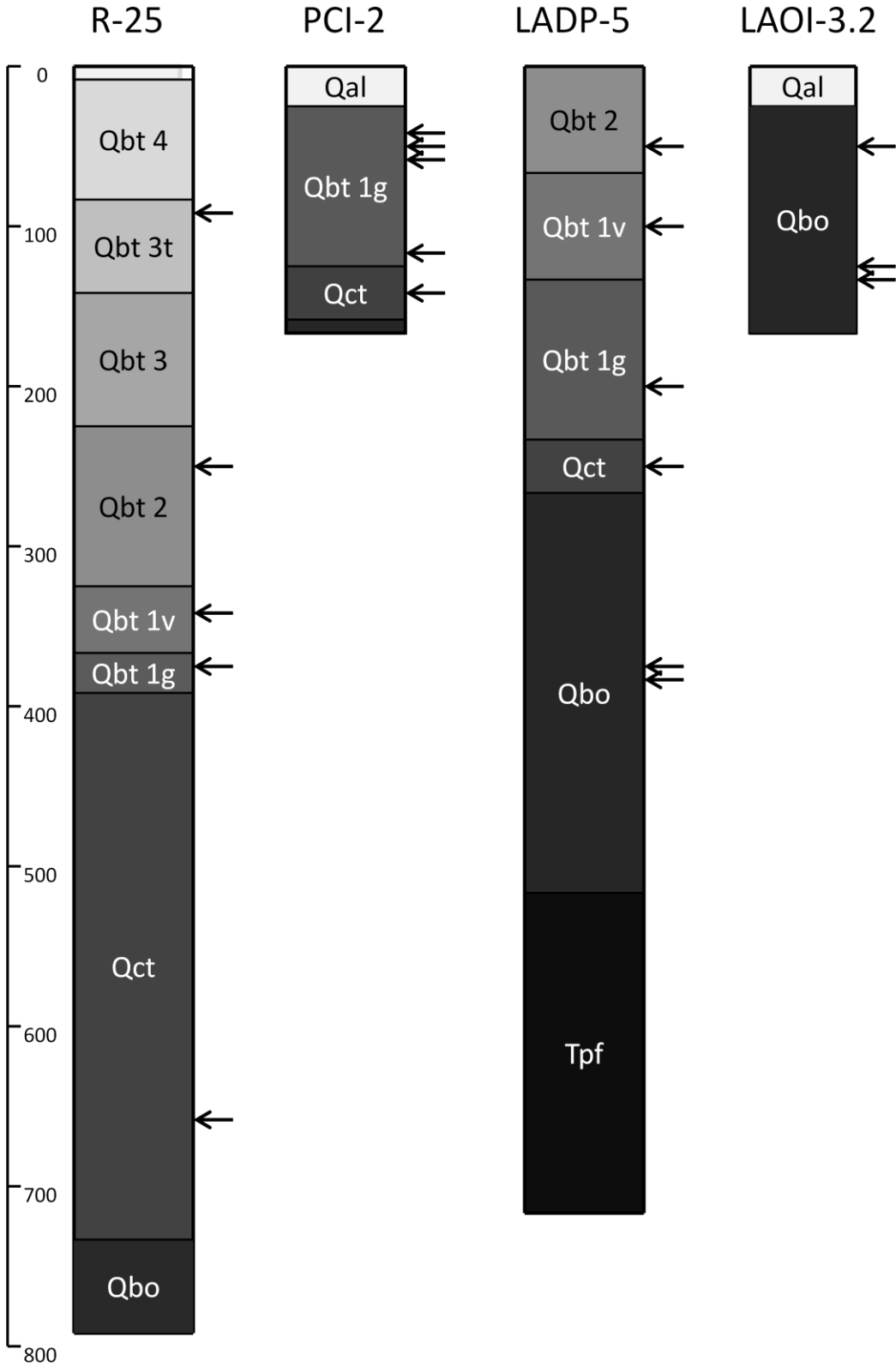
Figure 11: Gamma-ray logs from boreholes
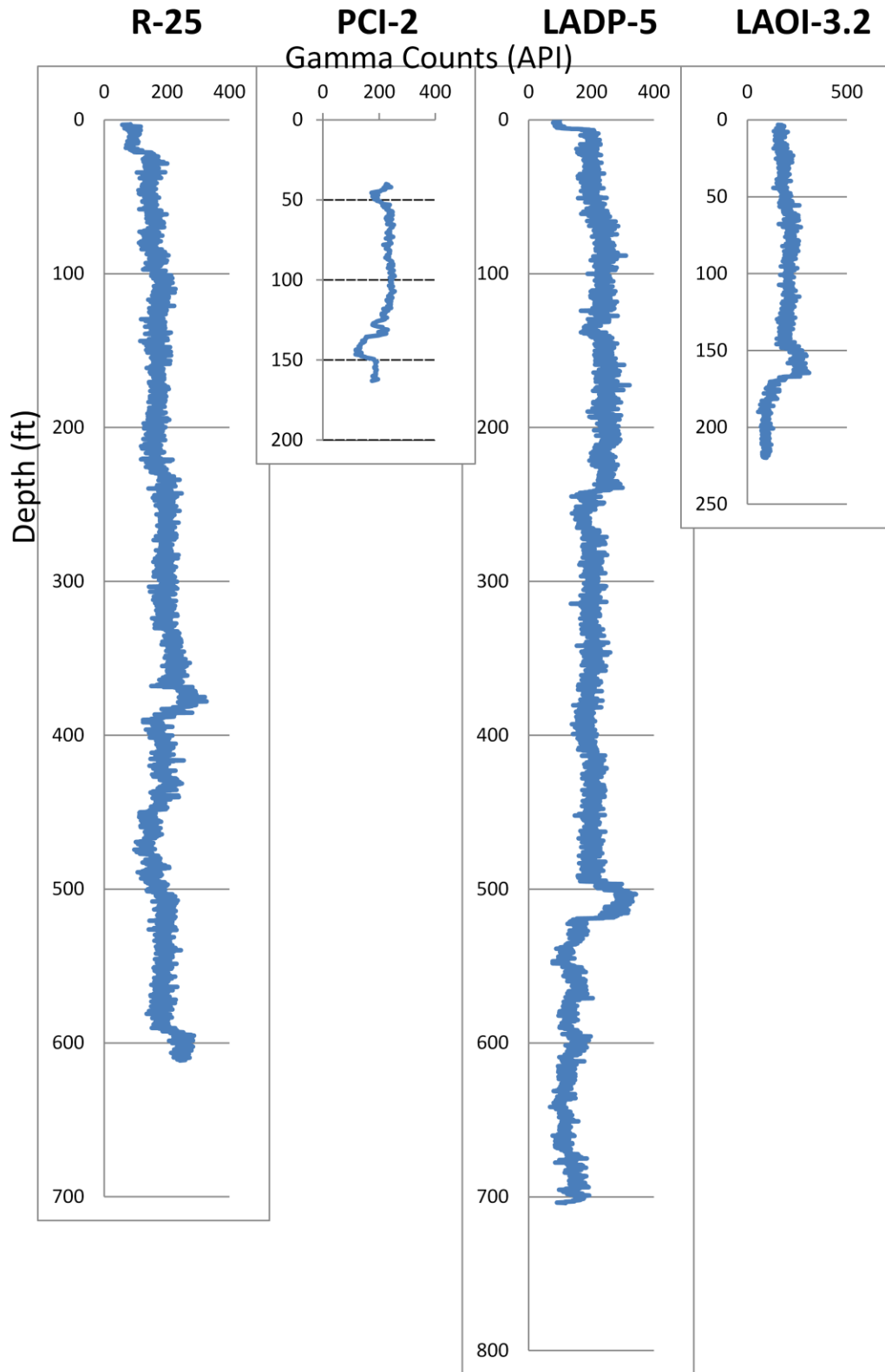
Figure 12: Reistivity logs from boreholes
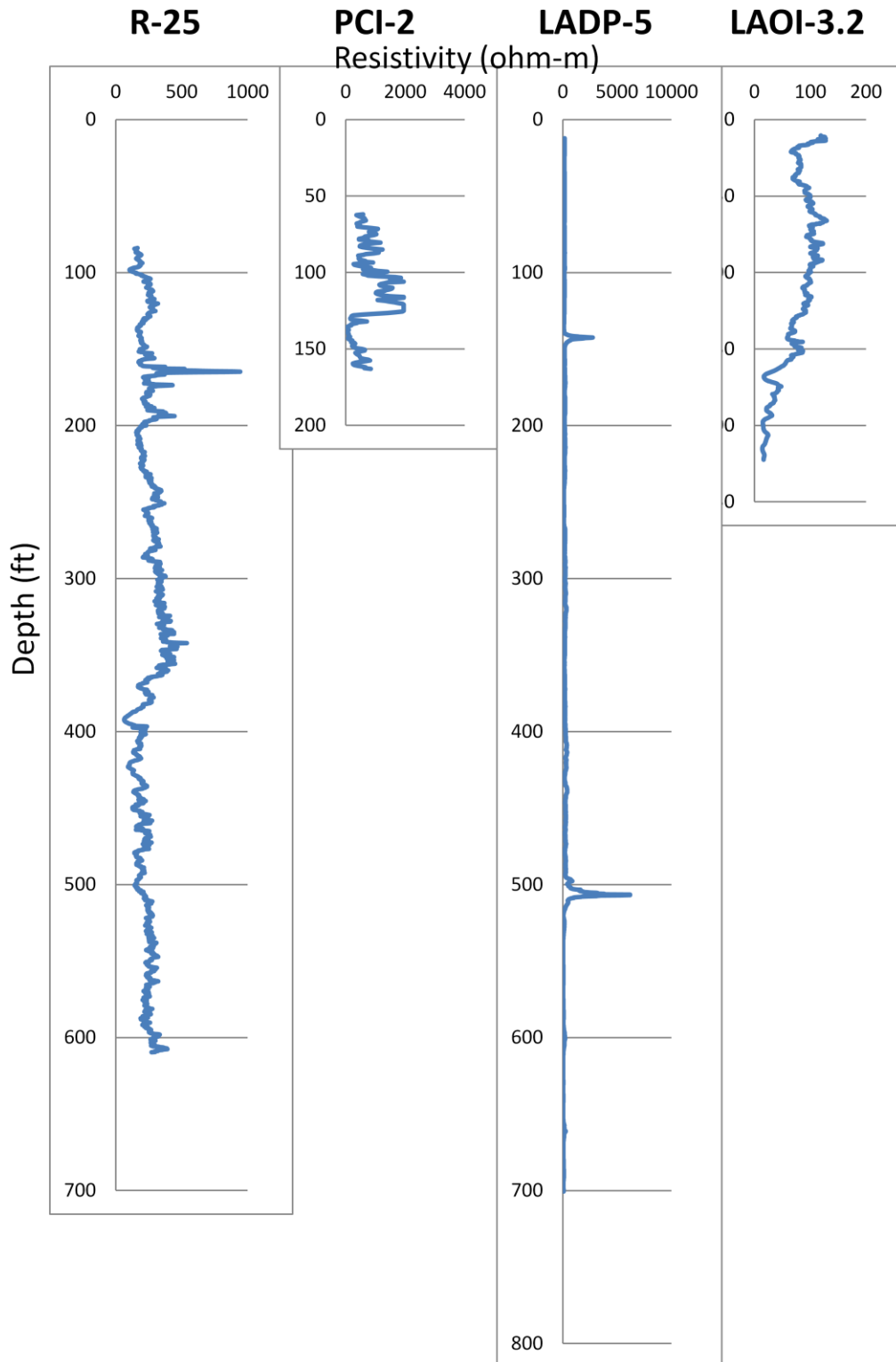
Figure 13: Plot comparing resistivity to distance from Pajarito Fault.
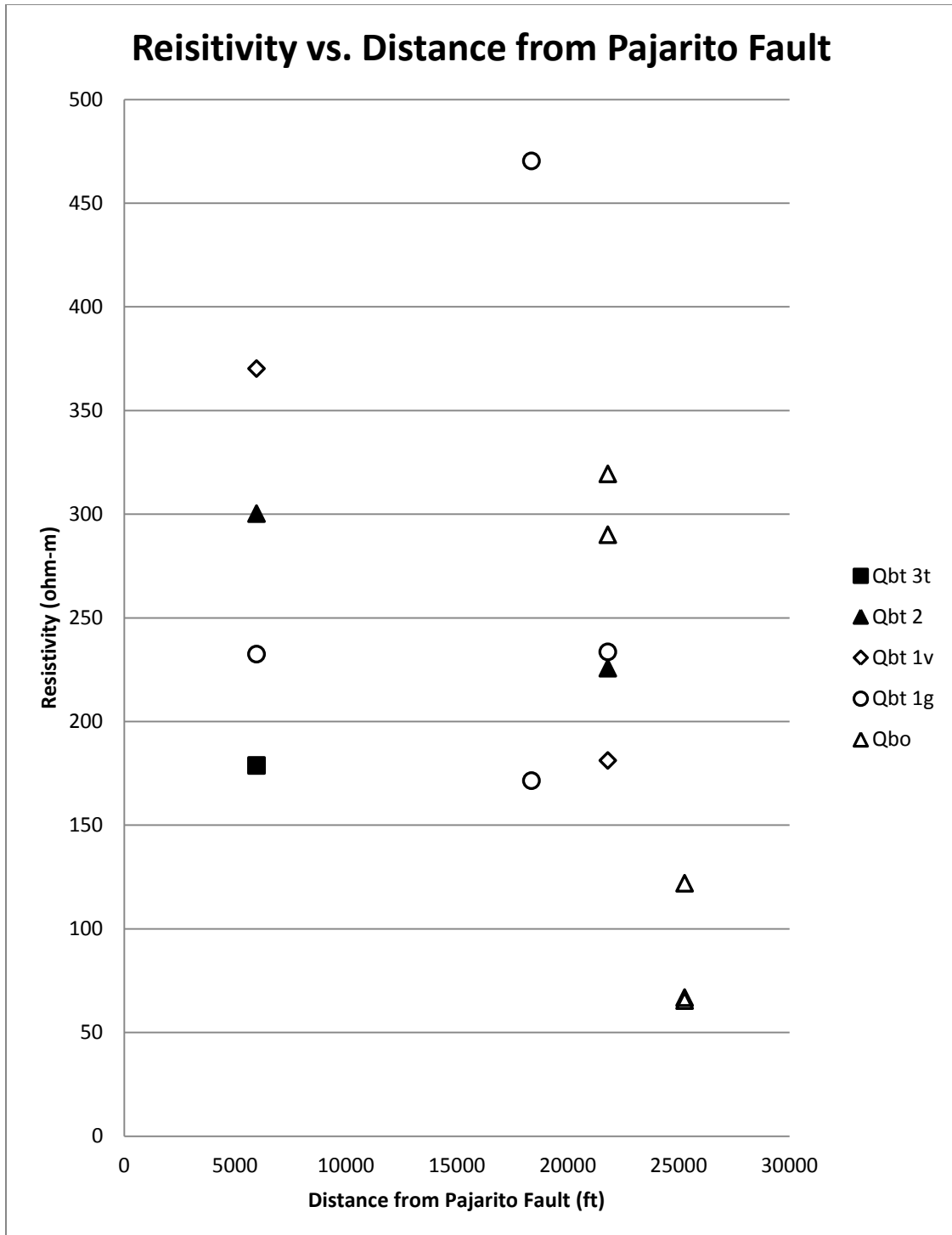
Figure 14: Plot comparing porosity to distance from the Pajarito Fault

Porosity vs. Distance from Pajarito Fault
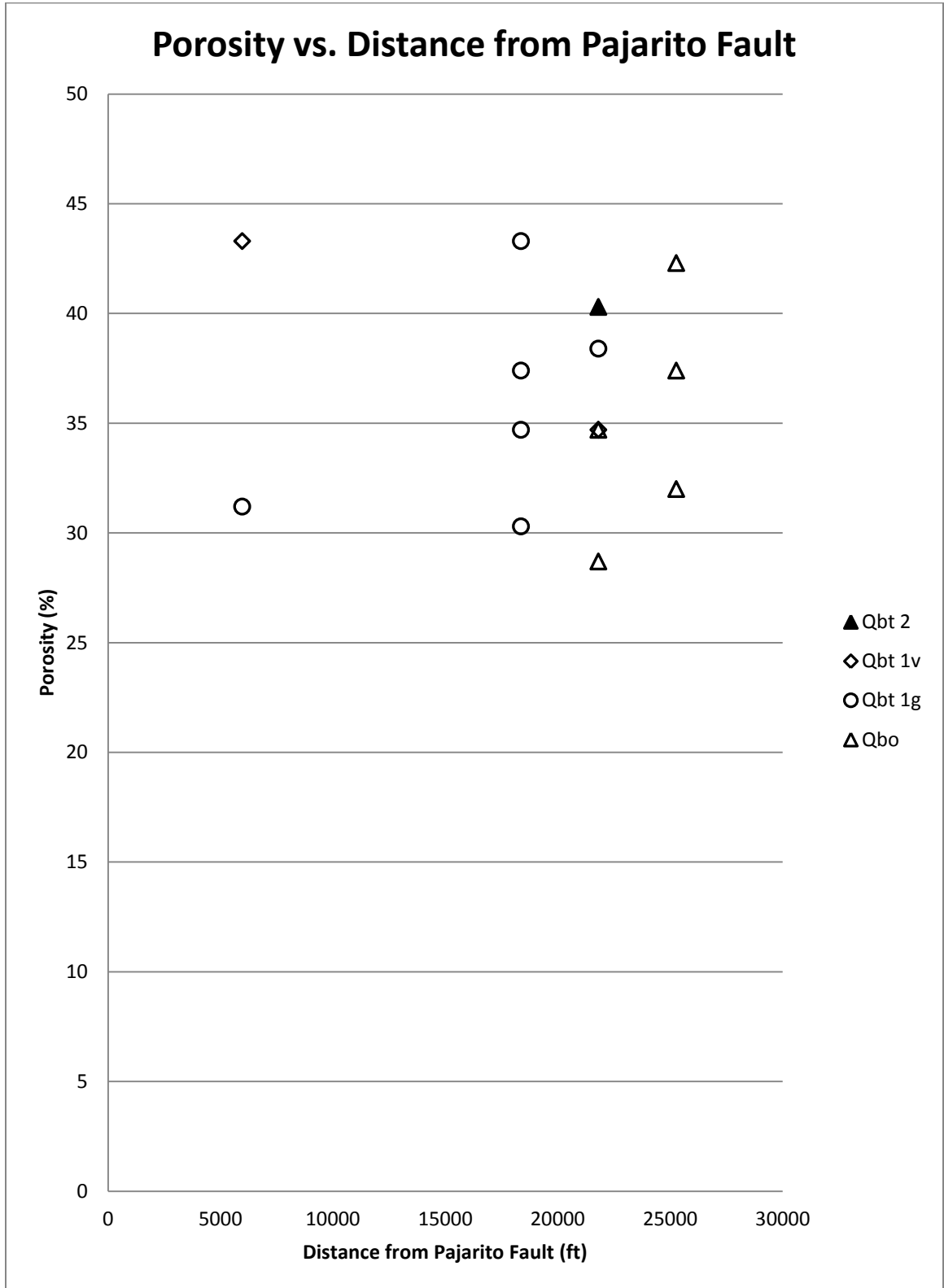
Figure 15: Plot comparing Saturated Hydraulic Conductivity vs. Distance from Pajarito Fault